Atmos. Chem. Phys. Discuss., 14, 27731–27767, 2014
www.atmos-chem-phys-discuss.net/14/27731/2014/
doi:10.5194/acpd-14-27731-2014

Atmospheric Chemistry and Physics Discussions

Long term measurements of optical properties and their hygroscopic enhancement

M. Hervo[1,*], K. Sellegri[1], J. M. Pichon[1], J. C. Roger[1], and P. Laj[2]

[1]Laboratoire de Météorologie Physique, CNRS UMR6016, Observatoire de Physique du Globe de Clermont-Ferrand, Université Blaise Pascal, Clermont-Ferrand, France
[2]Laboratoire de Glaciologie et Geophysique de l'Environnement, Universitée de Grenoble, CNRS, Grenoble, France
[*]now at: Federal Office of Meteorology and Climatology, MeteoSwiss, 1530 Payerne, Switzerland

Received: 18 September 2014 – Accepted: 24 September 2014 – Published: 6 November 2014

Correspondence to: K. Sellegri (k.sellegri@opgc.cnrs.fr)

Published by Copernicus Publications on behalf of the European Geosciences Union.

Abstract

Optical properties of aerosols were measured from the GAW Puy de Dôme station (1465 m) over a seven year period (2006–2012). The impact of hygroscopicity on aerosol optical properties was calculated over a two year period (2010–2011). The analysis of the spatial and temporal variability of the optical properties showed that while no long term trend was found, a clear seasonal and diurnal variation was observed on the extensive parameters (scattering, absorption). Scattering and absorption coefficients were highest during the warm season and daytime, in concordance with the seasonality and diurnal variation of the PBL height reaching the site. Intensive parameters (single scattering albedo, asymmetry factor, refractive index) did not show such a strong diurnal variability, but still indicated different values depending on the season. Both extensive and intensive optical parameters were sensitive to the air mass origin. A strong impact of hygroscopicity on aerosol optical properties was calculated, mainly on aerosol scattering, with a dependence on the aerosol type. At 90 % humidity, the scattering factor enhancement ($f\sigma_{sca}$) was more than 4.4 for oceanic aerosol that have mixed with a pollution plume. Consequently, the aerosol radiative forcing was estimated to be 2.8 times higher at RH = 90 % and 1.75 times higher at ambient RH when hygroscopic growth of the aerosol was considered. The hygroscopicity enhancement factor of the scattering coefficient was parameterized as a function of humidity and air mass type.

1 Introduction

Atmospheric aerosols directly interact with the solar radiation by scattering and absorption processes. This affects the visibility in all major urban areas but it also impacts global climate. The direct radiative effect (or Radiative Forcing for aerosol-radiation interaction *RFari* in IPCC 2013) depends on the aerosol optical properties. Long term studies of in situ aerosol optical properties measured over than more than one decade

ACPD
14, 27731–27767, 2014

show that there is no real trend on a global scale since 2000 (Collaud Coen et al., 2013). High altitude measurements are especially important as they are more representative of the global atmosphere than measurements at low altitude sites, especially for satellite validation (Laj et al., 2009). These sites are usually exempt from local pollution sources. Moreover high wind speeds, are frequently present in the free troposphere and transport the aerosols injected in this layer over long distances (Mattis et al., 2008; McKendry et al., 2007). Despite the importance of measurements at high altitude sites, there are currently only a small number of sites that perform continuous measurements of aerosol optical properties (Collaud Coen et al., 2007; Marcq et al., 2010). Andrews et al. (2011) presents a climatology of aerosol properties measured at the main altitude sites, among which two are located in Europe (the Junfraujoch station in Switzerland and the Monte Cimone station in Italy). These long-term datasets report dry measurements, while in the real atmosphere particles are subjected to atmospheric humidities ranging from 20 to 100 % and readily absorb water. Consequently, their size, chemical composition and optical properties change with humidity (Tang, 1996; Zhang et al., 2008). According to a recent study, water uptake on aerosol particles can be responsible of nearly 70 % of their total optical depth (Zhang et al., 2012). Therefore, hygroscopicity is a major parameter for the determination of optical properties and the direct radiative effect of aerosols (Pilinis et al., 1995; Yu et al., 2012).

To our knowledge there are only a few measurements of the impact of hygroscopicity on aerosol optical properties. The first laboratory measurements of the impact of water uptake on aerosol scattering was performed by Covert et al., in 1972. The first field studies on the impact of the hygroscopicity of ambient aerosols on aerosol optical properties was reported by Li-Jones et al. (1998), followed by measurements in the United States (Gassó et al., 2000; Kotchenruther et al., 1999), in Brazil (Kotchenruther and Hobbs, 1998) and in the South of Europe (Carrico et al., 2000). These type of studies are useful to compare in situ and remote sensing measurements at ambient humidities (Raut and Chazette, 2007; Zieger et al., 2011, 2012). In addition to the low number of in-situ measurements, the hygroscopic growth and subsequent modifica-

ACPD
14, 27731–27767, 2014

tion of the aerosol optical properties are still poorly quantified in global climate models (Ward and Cotton, 2011). Recently, through the use of Mie code, the impacts of hygroscopicity was estimated, not only on scattering and extinction, but also on other optical parameters such a the single scattering albedo or asymmetry factor (Adam et al., 2012; Fierz-Schmidhauser et al., 2010a, b; Schladitz et al., 2011; Zieger et al., 2010). The subsequent impact of hygroscopicity on the direct radiative impact was evaluated by Fierz-Schmidhauser et al., (2010a) and Stock et al. (2011). However, these later studies were performed over short-term periods, without taking into account the seasonal or pluri-annual variations. In the present study, both optical and hygroscopic properties were measured over several years at the high altitude Puy de Dôme station, and were used to characterize the impact of hygroscopicity on the optical properties of ambient aerosol particles and on their radiative effect.

2 Instrumentation and methodology

2.1 Sampling site and inlet

The Puy de Dôme station (PdD) is situated in the center of France (45.7723° N, 2.9658° E) at the top of a volcano (1465 m above sea level). Its altitude allows sampling in the boundary layer during the warm season and daytime, and in the free troposphere/residual layer during the cold season and nighttime (Venzac et al., 2009). According to Henne et al. (2010), the site is representative of western European air masses over a large scale. The PdD is mainly influenced by western winds and during the winter is in cloud 50 % of the time (RH > 98 %). At the PdD site aerosol measurements are performed behind a whole air inlet (RH < 40 %) with an upper cut-off diameter of 30 µm at average wind speeds, allowing the characterization of the whole aerosol population (interstitial and residual particles) during both clear and cloudy conditions.

ACPD
14, 27731–27767, 2014

2.2 Instrumentation and method

The scattering (σ_{sca}) and backscattering coefficients were measured at 3 wavelengths from July 2006 to December 2012 using a nephelometer TSI 3563. Corrections for detection limits and truncation errors were applied according to Anderson and Ogren (1998). The Angstrom exponent (α) was calculated between 450 and 700 nm. The asymmetry parameter (g) was calculated from the backscatter ratio measured by the nephelometer following the parameterization of Andrews et al. (2006). The absorption coefficient (σ_{abs}) was measured by a Multi Angle Absorption Photometer (MAAP 5012), with a central wavelength of 637 nm (Petzold et al., 2005) from January 2008 to December 2012. Between July 2001 and December 2008, an aethalometer AE16 from Magee Scientific was measuring the absorption at 880 nm. The aethalometer is known to overestimate σ_{abs} (Arnott et al., 2005; Collaud Coen et al., 2010; Schmid et al., 2006), and although different correction procedures exist there is no consensus available on the best way to correct the Aethalometer measurements (Collaud Coen et al., 2010; Virkkula et al., 2007; Weingartner et al., 2003). Both instruments were running side by side during 2008, showing a good correlation over this period ($r^2 = 0.82$). The combination of the scattering and absorption coefficients allowed us to calculate the extinction coefficient (σext) and the single scattering albedo $\omega 0$. The absorption at 550 nm was extrapolated from measurements at 637 nm with an absorption Angstrom exponent of 1. More information about these instruments and error calculations are discussed by Hervo et al. (2012). The particle size distributions of aerosols with diameters between 10 to 500 nm were measured by a Scanning Mobility Particle Sizer (SMPS, Wiedensohler et al., 2012) between December 2005 and December 2012. For particle diameters between 300 nm and 20 µm, an Optical Particle Counter (OPC, Grimm, model 1.108, Burkart et al., 2010) was operating at the site from February 2010 to December 2012. For each measurement, the complete size distribution (merged between SMPS and OPC) was fitted by 3 lognormal modes (nucleation, accumulation

ACPD
14, 27731–27767, 2014

and coarse mode). The diameter and the SD of each mode was fitted with a least square method.

The hygroscopicity of the particles was measured at 90 % RH by an Hygroscopic Tandem Differential Mobility Analyser (HTDMA, Villani et al., 2008). The growth factor (GF) was calculated as the ratio between wet and dry diameters. The HTDMA measurements were sorted into 3 modes: hydrophobic, hygroscopic and very hygroscopic after a log-normal fitting procedure on the hygroscopic growth factor distribution, according to Holmgren et al. (2014). The HTDMA was involved in international intercomparisons for the European project EUSAAR (European Supersites for Atmospheric Aerosol Research) showing that the uncertainty in the growth factor is less than 2 % for the PdD HTDMA instrument (Duplissy et al., 2009). Diffusion, absorption, hygroscopic growth and submicron size distribution measurements were performed according to the requirements of the ACTRIS European Infrastructure project.

In order to calculate the refractive index, the scattering and the absorption values were first computed using a Mie code (Bond et al., 2006; Mätzler, 2002) with an a priori refractive index ($1.55 + 0.05i$). The refractive index was then modified iteratively until the measured extinction fits the calculated one. This method was described for the first time by Raut and Chazette (2007). It has been used in different studies for computing complex optical properties like the refractive index or the Lidar ratio (e.g. Bukowiecki et al., 2011; Hervo et al., 2012)

All wet optical properties and enhancement factors were calculated from the calculated wet size distributions and wet refractive index using a Mie code. The wet size distribution was computed from the hygroscopic growth factor, retrieved from the HTDMA measurements at 110 nm, applied to each size mode measured by the SMPS. The modification of the wet refractive index (i.e. after the hygroscopic growth was applied) was calculated using the volume weighted mixing rule (Hasan and Dzubay, 1983; Michel Flores et al., 2012).

This is not direct measurements but approximations using synergetic measurements of 5 instruments. Zieger et al. (2013) recommended this method to calculate

ACPD
14, 27731–27767, 2014

the scattering enhancement factor (f(RH)) when no direct measurements are available. Zieger et al. (2013) demonstrated that, on average, the calculation using HTDMA and size distribution (submicron) agreed with direct measurements (sub- and super-micron) with less than 10 % discrepancy (e.g. at the altitude station Jungfraujoch: $f_{pred}/f_{meas} = 1.07 \pm 0.12$, including instrument systematic error). However, they clearly mentioned that "standard HTDMA may miss the important coarse mode contribution to f(RH) and therefore may under- or over-estimate the overall f(RH)".

In our work we also may under- or over-estimate the overall f(RH) due to the assumption of a constant chemical composition between accumulation and coarse mode, in case of a super-micron dust or sea salt, respectively. Like suggested by Zieger et al. (2013) this error is estimated to be, in average, less than 10 %.

The structure of the atmosphere strongly influences measurements performed at high altitude stations. Hence, the height of the planetary boundary layer was calculated with a Raymetrics Lidar measuring at 355 nm (Hervo et al., 2012). The Lidar was installed at 425 m a.s.l. at 11 km from the PdD (45.76° N, 3.11° E). The vertical resolution was 7.5 m. The boundary layer was defined as the first mixed layer of aerosol. This height was calculated using a Wavelet Covariance Transform (WCT) algorithm (Baars et al., 2008; Brooks, 2003). Optical depth measurements were obtained from a Cimel CE-318 sunphotometer, installed next to the Lidar. The sun photometer measures the aerosol optical depth at 4 different wavelengths (440, 670, 870, 1020 nm) and various optical properties (such as the phase function, refractive index or single scattering albedo...) were obtained by performing the almucantar inversion (Dubovik and King, 2000). The data were processed and quality assured by AERONET (Aerosol Robotic Network) network.

ACPD
14, 27731–27767, 2014

3 Dry optical properties

3.1 Temporal variations

3.1.1 Scattering coefficient

The mean scattering coefficient (σ_{sca}) at PdD calculated over the period 2008 to 2012 (mean: 19.5 Mm^{-1}, median 12.2 Mm^{-1}, SD 25.8 Mm^{-1}, 90th percentile 43.6 Mm^{-1}) was lower than the mean scattering coefficient reported at other low altitude sites in Europe. For example, in Granada, Spain the mean value was 60 ± 30 Mm^{-1} (Lyamani et al., 2010) or in eastern Europe: 40 ± 27.1 Mm^{-1} (Kalivitis et al., 2011). Values measured at PdD were closer to those at high altitude sites, where median values of around 10 Mm^{-1} were measured for both Izaña and Monte Cimone (Andrews et al., 2011). A Mann Kendall test (Gilbert, 1987) applied to the measurement period shows that no pluri-annual trend can be observed. The lack of a pluri-annual trend was similarly observed at different high altitude sites in Europe, such as the Jungfraujoch (3580 m) in Switzerland or Hohenpeissenberg (950 m) in Germany (Collaud Coen et al., 2012).

Figure 1 shows the diurnal variations of the optical properties for the different seasons. A clear seasonal variability of the scattering coefficient is shown in Fig. 1a), with a maximum σ_{sca} in spring, followed by summer, autumn and a minimum in winter. These observations are coherent with the observations reported at other high altitude stations (Andrews et al., 2011). Nevertheless the seasonal variations are opposite to the ones observed at boundary layer sites such as Granada, where maximum values were reported during winter (Lyamani et al., 2010). At boundary layer sites the diurnal variation showed (Fig. 1a) a σ_{sca} maxima measured during the day, between 12:00 UTC (spring and summer) and 15:00 UTC (autumn and winter). For altitude stations in general and for the PdD station in particular, the diurnal and seasonal variations are likely to be linked to the height of the Planetary Boundary Layer (PBL). Indeed, LIDAR PBL retrievals showed that in summer or during the day, the PBL was higher than during winter and at night, so that altitude sites were more influenced by surface emissions

ACPD
14, 27731–27767, 2014

when they were within the PBL. During the night or winter, the site was mostly influence by the free troposphere or residual layer (Fig. 2).

3.1.2 Absorption coefficient

The absorption coefficient has been measured at PdD site since 2001, making it one of the longest dataset of optical properties available at PdD. The order of magnitude of σ_{abs} median value (0.80 Mm^{-1} [25th percentile: 0.09–75th percentile 3.42] during night and 1.28 Mm^{-1} [0.17–4.72] during day (also given in Table 1) was very similar to the σ_{abs} reported for other high altitude stations in Europe (Jungfraujoch and Izana: $\sim$ 0.5 Mm^{-1}, Monte Cimone 2 Mm^{-1} Andrews et al., 2011). Similar to the scattering coefficient, no significant pluri-annual trend was observed. On Fig. 1b the absorption coefficient shows clear seasonal and diurnal variations. σ_{sca} and σ_{abs} were strongly impacted by the boundary layer dynamics, with maximum values when the boundary layer reaches the PdD altitude, i.e. during the summer and at daytime.

3.1.3 Intrinsic optical properties

Unlike the scattering and absorption coefficient, single scattering albedo ($\omega 0$) and asymmetry factor (g) only depend on the aerosol type, and not on the aerosol concentration. The median single scattering albedo at PdD (Table 1) was close to the one measured at other high altitude sites (0.90±0.05, Andrews et al., 2011). In urban areas, particles were more absorbing and $\omega 0$ was generally lower (e.g. 0.68 ± 0.07, Lyamani et al., 2010). At PdD, no pluri-annual variability was observed in the time period from 2006 to 2012. However, $\omega 0$ shows a seasonal variation with minimal values during winter and highest values during summer (Fig. 1). Therefore, the fraction of absorbing aerosols was higher during winter. This can be explained by different factors. First, the proportion of combustion aerosols, which were more absorbing, were expected to be higher during winter. Second, purely scattering aerosols were larger, and hence preferentially scavenged by clouds (Marcq et al., 2010) that were frequently at the site during

ACPD
14, 27731–27767, 2014

winter. Then, there was a reduced formation of secondary aerosols induced by a lower solar intensity during winter (Boulon et al., 2011). Lowest values were likely a result of a bias in the measurements induced by the very low aerosol concentration in winter. Similar seasonal variations were observed on most high altitude sites discussed by Andrews et al. (2011). A slight diurnal variation of $\omega 0$ was detectable with a lower value during the day, suggesting an increase in absorbing aerosols brought by the rising boundary layer, which contains a higher proportion of primary particles, mostly from combustion processes during winter.

The asymmetry factor (g), describing the scattering geometry, was calculated from nephelometer measurements from 2006 to 2012. At PdD, the median g was 0.57, which was the same order of magnitude than from other measurements performed in France close to Marseille (0.59 ± 0.05, Mallet et al., 2003), but lower than those measured at high altitude in Nepal (from 0.63 to 0.78, Marcq et al., 2010). A slight seasonal variability was perceptible, with a minimum in winter, but no daily variation was detectable. Andrews et al. (2006) suggested that the variation of g could be explained by changes in aerosol size distributions, in agreement with observations of Venzac et al. (2009), who observed a decrease in average particle diameters during winter but no variation between day and night at the PdD station.

A refractive index (m) was calculated for 2010 and 2011 when the SMPS, OPC, Nephelometer and MAAP instruments were running simultaneously. The median m calculated at PdD was $1.43 + 0.011i$ [$1.36 + 0.004i$ $1.55 + 0.04i$]. This value was slightly lower than the one calculated at the Jungfraujoch from the aerosol chemical composition, with a reported average refractive index of $1.52 + 0.03i$ (Fierz-Schmidhauser et al., 2010a). However, the refractive index reported by Fierz-Schmidhauser et al. (2010a) was calculated over a small period that might not be representative of the whole year. Indeed, the refractive index calculated from in situ measurements showed a significant seasonal variation, with a higher real and imaginary refractive index during winter (Fig. 1e and f). This points to the lack of representativeness of refractive indexes calculated over short periods. A higher real and imaginary refractive index during winter was

ACPD
14, 27731–27767, 2014

coherent with the hypothesis of a higher proportion of combustion aerosol during winter, even though no clear dinurnal variation was visible. This is likely because the refractive index of black carbon is high (m_{BC} = 1.95+0.79i, Bond and Bergstrom, 2006), From our data set, the in-situ refractive index was compared with data from the co-localized sunphotometer, during non-cloudy daytime periods. The median m agrees within 4 % of the real part of the refractive index derived from the sun-photometer and within 40 % of its imaginary part. When ambient humidity was taken into account (wet refractive index calculated according to volume weighted mixing rule, Hasan and Dzubay, 1983; Michel Flores et al., 2012), the median of the refractive index agreed within 5 % of both the real and imaginary part of the refractive index.

At the PdD, several studies have shown that the physical and chemical characteristics of aerosols depend both on the time of the year and the time of the day, but also on the air mass type sampled at the site (Freney et al., 2011). The long data set acquired at PdD offers a unique chance to characterize both the temporal and spatial variability of the aerosol optical properties. In the following section, the spatial variations of these properties are analysed.

3.2 Spatial variations

Optical properties of aerosols depend on their size distribution and chemical composition, which in turn highly depend on their geographical origin (Bourcier et al., 2012; Venzac et al., 2009). Hence, it is essential to characterize the optical properties of particles according to the air mass type in which they were sampled. 72 h back trajectories were calculated every 6 h between 2008 and 2012 using the Lagragian model Hysplit (Hybrid Single-Particle Lagrangian Integrated Trajectory) (Draxler and Rolph, 2012).

Instead of separating the air mass types into discrete sectors, it was possible to attribute the aerosol optical properties to a given spatial origin along the trajectory pathway. Each 6 h average sampled at PdD was associated to a portion of the corresponding back trajectory, with a decreasing weight as the distance (time) from the sampling point increases. Resulting maps for the optical properties are shown in Fig. 3.

ACPD
14, 27731–27767, 2014

The scattering coefficient showed a clear spatial variability. The σ_{sca} of aerosols representative of eastern continental air masses was strongly in contrast with the σ_{sca} of aerosol in western oceanic air masses. The scattering coefficient was higher for particles transported by continental air masses, mainly from anthropogenic sources. σ_{sca} was particularly low for oceanic air masses, which contain lower aerosol concentrations (Bourcier et al., 2012; Venzac et al., 2009). A very similar behaviour was observed for the absorption coefficient with high σ_{abs} from the central and eastern European part, and low σ_{abs} from the Atlantic Ocean. The single scattering albedo presented a smaller west–eastern gradient, suggesting that, in proportion to the total aerosol mass, the oceanic aerosol contained a higher absorbing fraction than over continental areas. This result could be surprising, as strongly absorbing anthropogenic aerosols such as black carbon are mainly emitted over continental Europe. This feature was confirmed by analysing the absolute values of absorption and scattering coefficients. Indeed, aerosols form continental Europe were more absorbing ($\sigma_{abs} \approx 3\,Mm^{-1}$) than oceanic aerosols ($\sigma_{abs} \approx 1\,Mm^{-1}$). However the difference was even stronger for the scattering coefficient between continental ($\sigma_{sca} \approx 25\,Mm^{-1}$) and oceanic ($\sigma_{sca} \approx 5\,Mm^{-1}$) air masses. Moreover, when particles coming from Eastern Europe were measured at PdD, they travelled over long distances and absorbing soot may have experienced a substantial ageing. This ageing resulted in the condensation of less absorbing species such as ammonium sulphate.

The asymmetry coefficient also showed an increasing west–eastern gradient. The variability of g was explained by a combination of size and refractive index evolutions. Hence the spatial variation of this parameter was difficult to interpret. The refractive index was calculated only when the data of 4 instruments were simultaneously available (SMPS, OPC, MAAP and nephelometer), implying a lower temporal coverage and less statistical reliability for this parameter. However the refractive index was calculated for each type of air masses, with no significant difference between air masses (Table 1).

In order to compare these results with values reported in the literature for others stations, the air masses sampled at PdD are classified under 5 categories: African,

ACPD
14, 27731–27767, 2014

continental, local, oceanic and oceanic modified (Fig. 5). Air masses sampled at the PdD station originated in majority from the oceanic sector (37.8 % over the calculation period), while African, continental and oceanic modified air masses represented 27.1, 18.4 and 20 % of the air mass types, respectively. Local air masses were scarce (7.2 %). The year-to-year variability of the origin of air masses was not substantial, but the seasonal variation was noteworthy. The continental air masses were nearly absent during July and August. They were mainly replaced by oceanic air masses. Finally, the origin of the air mass was mainly constant during the day (not shown).

The main optical properties are summarized in Table 1.

Table 1 summarizes the features highlighted from the analysis of the maps (Fig. 3) with σ_{sca} and σ_{abs} 3.2 and 3.8 times higher for continental and local air masses compared to oceanic air masses, respectively. As the result of the diurnal variation of the boundary layer height, a clear diurnal variation for the absorption and scattering coefficients was observed whatever the air mass origin. While daytime values may be compared to boundary layer sites, night-time values can be compared to high altitude sites.

As already mentioned for the whole data set, within a given air mass, the diurnal and spatial variation of the single scattering albedo were less contrasted than for σ_{sca} and σ_{abs}, except during the day for local air masses, where fresh emissions induced a lower $\omega 0$.

In this section, an overview of the evolution of the dry optical properties of aerosols over a relatively large period of time and relatively large spatial scale was given. In the following section, the impact of the water presence on aerosols on their optical and radiative properties was quantified over temporal and spatial scales.

4 Wet optical properties

The hygroscopicity of aerosols may strongly influence their optical properties, and in particular aerosol scattering ability. This impact was characterized by calculating the

ACPD
14, 27731–27767, 2014

enhancement factor (f(RH)) of the scattering coefficient at a given relative humidity (RH). This f(RH) was defined as the ratio between the wet and the dry scattering coefficient. f(90 %) has been calculated from PdD measurements on more than 1000 3 h averaging periods in 2010 and 2011 and averaged to monthly means (Fig. 4). Due to instrumental failures, no measurements were available in January and August of both years. However, f(90 %) shows a marked seasonal variation with maximum enhancements during the warm season.

No clear diurnal variation of f(90 %) was observed, indicating that the boundary layer height was not a major parameter influencing the seasonal variation observed, and that the seasonal variation of the air mass types is driving this variability. In order to apply a humidity enhancement factor at ambient relative humidities and for given aerosol types, f(RH) was parameterized for the different aerosol origins discriminated within our data set. From the measurements of the growth factor at 90 %, the growth factor was extrapolated between 10 and 95 % using the kappa theory (Petters and Kreidenweis, 2007). Then the wet size distribution and the wet refractive index were used to calculate f using a Mie code (Fig. 5).

Median values calculated for discrete RH were fitted with the sum of 2 exponentials (Eq. 1), which parameters are summarized Table 2. This parameterization can be used to estimate wet optical properties when no hygroscopic measurements are available. The calculated f humidograms did not take into account the deliquescence and efflorescence of aerosols. This was supported by the fact that enhancement factors humidograms given in the literature for directly measured ambient atmospheric aerosols using the wet nephelometer technique did not show any deliquescence point (Fierz-Schmidhauser et al., 2010a; Zieger et al., 2011) except for clean marine air masses (Fierz-Schmidhauser et al., 2010b).

$$f\sigma_{550} \approx a_1 e^{a_2 \mathrm{RH}} + a_3 e^{a_4 \mathrm{RH}} \quad (1)$$

Clear differences between the parameterizations obtained in different air masses were observed. The lowest f was observed for continental air masses (f(90 %) = 2.56±1.86).

ACPD
14, 27731–27767, 2014

Figure 5 shows, that this was in good agreement with values measured at Ispra, Italy ($f(90\%) = 2.10$ [1.58–3], Adam et al., 2012), defined as a polluted continental site, and for polluted air masses at Mace Head, Ireland ($f(85\%) = 1.77 \pm 0.31$, Fierz-Schmidhauser et al., 2010b). It was also in good agreement with results obtained in the south of Portugal for polluted air mass ($f(82\%) = 1.46 \pm 0.1$, Carrico et al., 2000).

A second range of hygroscopic scattering enhancement factors appeared for aerosols representative of oceanic, African and local air masses. The values of $f(90\%)$ for these aerosol types were higher than for aerosols in continental air masses (respectively 2.93 ± 1.45, 2.89 ± 1.52 and 2.8 ± 1.03). In Fig. 5, the value of f for oceanic air mass at PdD was close to the one measured at Mace Head for air masses from the clean sector ($f(85\%) = 2.22 \pm 0.17$, Fierz-Schmidhauser et al., 2010b). For a Saharan dust event, f measured at the Jungfraujoch high altitude site ($f(85\%) = 1.72$, Fierz-Schmidhauser et al., 2010a) was close to the one observed for African air masses at PdD. At the Cape Verde station, aerosols mainly originated from marine and Saharan origins, $f(90\%)$ and had an average value of 2.55 (Schladitz et al., 2011).

Finally, f was highest for the air masses from the oceanic modified origin ($f(90\%) = 4.36 \pm 2.51$). Zieger et al. (2010) reported a similar value in the Arctic ($f(85\%) = 3.24 \pm 0.53$). Zieger et al. highlighted that f was highly dependent on the particles' hygroscopicity, but also on the particle dry size. Indeed, for a given chemical composition, f strongly decreased with an increasing diameter. Hence, f was higher for particles of lower hygroscopicity and of smaller diameters than sea salt. Particles in modified air masses were smaller compared to oceanic air masses, as shown by their respective angstrom coefficient, which may explain why f was larger in modified oceanic air masses than in purely oceanic air masses.

At the high altitude site of Jungfraujoch (Fierz-Schmidhauser et al., 2010b), the order of magnitude and the variability of $f(85\%) = 2.23$ [1.3 3.3] in all air masses together, over a month of measurements, was similar to the average and variability observed for the Puy de Dôme site. Other studies outside Europe reported $f(80–85\%)$ values ranging from 1.8 to 2.54 for marines aerosols, from 1.58 for polluted marines aerosols,

ACPD
14, 27731–27767, 2014

from 1.4 to 1.65 for anthropogenic aerosols, from 1.0 to 1.13 for dust and finally from 1.1 to 1.4 for particles freshly emitted by biomass burning (Stock et al., 2011 and references included). These values are consistent with our measurements.

As the water is not an absorbent material, the impact of hygroscopicity on the absorption coefficient was limited. Some studies considered that the water uptake effect was negligible (Nessler et al., 2005; Zieger et al., 2010, 2011), others highlight a small enhancement with humidity: 1.1 at Ispra (Adam et al., 2012) or 1.043 at Cape Verde (Schladitz et al., 2011). The impact of hygroscopicity on the absorption coefficient was quantified from our measurements, confirming the low enhancement factors with humidity of the absorption coefficient (see Table 3). The effect of humidity on the extinction and on the asymmetry factor was also rather low (on average less than 15 %), but could nevertheless impact the aerosol radiative impact.

5 Radiative effect

The aerosol direct radiative effect was estimated with a simple radiative transfer model, using the two flux approach from Chylek and Wong, (1995). From this approximation, the direct radiative forcing at the top of the atmosphere was calculated with:

$$\Delta F = -\frac{S_0}{2} T_{\mathrm{atm}}^2 (1 - N_{\mathrm{cloud}}) \left[(1-a)^2 \beta_{\mathrm{r}} \omega 0 - 2a(1 - \omega 0) \right] \tau \quad (2)$$

With S_0 the solar constant, T_{atm} the transmittance of the atmosphere above the aerosol layer, N_{cloud} the cloud fraction, a the surface albedo (0.16), τ the optical depth, $\omega 0$ the single scattering albedo and β_{r} the fraction of radiation scattered to the upper part of the atmosphere. The values of ΔF were calculated for a clear sky, i.e. for N_{cloud} equals to zero. β_{r} was approximated by $\beta_{\mathrm{r}} = 0.5(1 - g)$ with g the asymmetry factor calculated from the nephelometer.

ACPD
14, 27731–27767, 2014

This approach was frequently used in the literature (e.g. Andrews et al., 2011; Bond and Bergstrom, 2006; Cheng et al., 2008; Delene and Ogren, 2002; Lesins et al., 2002; Stock et al., 2011).

In order to estimate the impact of hygroscopicity on the direct radiative forcing of aerosols, the hygroscopic radiative forcing ratio ($f\Delta F$) was defined as the ratio of the radiative impact calculated at a RH of 90 % (ΔF_w) to the one calculated in dry conditions (ΔF_d). $f\Delta F$ was calculated with the following equation:

$$f\Delta F = \frac{\left[(1-a)^2\beta_{r_w}\omega 0_w - 2a(1-\omega 0_w)\right]\tau_w}{\left[(1-a)^2\beta_{r_d}\omega 0_d - 2a(1-\omega 0_d)\right]\tau_d} \quad (3)$$

The subscripted index "w" was used for wet measurements and "d" for dry measurements. In case of an homogenous atmospheric layer, the ratio between wet and dry optical depths was equal to the ratio between wet and dry extinction coefficients. $f\Delta F$ was calculated at 90 % humidity for all the available measurements in 2010 and 2011. The median $f\Delta F$ calculated from PdD measurements are summarized in Table 4.

As the scattering enhancement strongly influences $f\Delta F$, the results were close to the ones shown in Fig. 5. The lowest $f\Delta F$ was detected for continental air masses. Larger values were detected for oceanic, African and continental air masses. The maximum values were observed for aerosols from oceanic modified origin, for which the radiative forcing calculated at 90 % was more than 4 times higher than for dry conditions.

6 Conclusions

From 2006 to 2012, the optical properties of aerosol particles were characterized at the Puy de Dôme station, 1465 m a.s.l., together with their change due to water uptake from 2010 to 2011. The analysis of the spatial and temporal variability of the optical properties showed that while no long term trend was found, a clear seasonal variation was

ACPD
14, 27731–27767, 2014

observed on the extensive optical parameters (scattering, absorption). Extensive parameters (scattering and absorption coefficients) showed a clear diurnal and seasonal variability. They were highest/maximal during the warm season and in the afternoon, when an efficient vertical mixing of the PBL reaches the site. Intensive parameters (single scattering albedo, asymmetry factor, refractive index) did not shown such a strong diurnal variability. These values may be useful as representative characteristics of the PBL and the nocturnal residual layer in Western Europe. Both extensive and intensive optical parameters were sensitive to the air mass origin.

This study highlights the significant impact of hygroscopicity on aerosol optical properties, and how this is influenced by aerosol type. In particular, the calculated scattering coefficient humidity enhancement factor (f) was the highest during summer, most likely due to a higher fraction of hygroscopic aerosols. f was highly dependent on the air mass type, with maximum values in modified oceanic air masses. Modified oceanic air masses contained high proportions of small hygroscopic aerosols. As a result, a parameterization of the scattering coefficient humidity enhancement factor was proposed as a function of relative humidity and air mass type. This parameterization can be used to estimate wet optical properties when no hygroscopic measurements are available. f measured at the PdD in different air mass types compared well with f measurements reported in the literature for specific places in Europe. It confirmed the representativeness of our measurements at the European scale. Hence, the parameterizations provided in the present work can be applied whenever the size distribution or the hygroscopicity of the aerosol is unknown.

Finally, using these results, the impact of hygroscopicity on the direct radiative effect of aerosols was evaluated. In case of highly hygroscopic oceanic modified air masses, the radiative forcing calculated at a relative humidity of 90 % was more than 4 times higher than for dry conditions.

Acknowledgements. The authors would like to acknowledge the OPGC and its staff and INSU-CNRS for their contribution to establishing and maintaining the PdD measurement site. This

ACPD
14, 27731–27767, 2014

work was performed in the frame of the european EUSAAR (R113-CT-2006-026140) and EUCAARI (0136 833-2) and the french ORAURE SOERE.

References

Adam, M., Putaud, J. P., Martins dos Santos, S., Dell'Acqua, A., and Gruening, C.: Aerosol hygroscopicity at a regional background site (Ispra) in Northern Italy, Atmos. Chem. Phys., 12, 5703–5717, doi:10.5194/acp-12-5703-2012, 2012.

Anderson, T. and Ogren, J.: Determining aerosol radiative properties using the TSI 3563 integrating nephelometer, Aerosol Sci. Tech., 29, 57–69, 1998.

Andrews, E., Sheridan, P. J., Fiebig, M., McComiskey, A., Ogren, J. A., Arnott, P., Covert, D., Elleman, R., Gasparini, R., Collins, D., Jonsson, H., Schmid, B., and Wang, J.: Comparison of methods for deriving aerosol asymmetry parameter, J. Geophys. Res., 111, D05S04, doi:10.1029/2004jd005734, 2006.

Andrews, E., Ogren, J. A., Bonasoni, P., Marinoni, A., Cuevas, E., Rodríguez, S., Sun, J. Y., Jaffe, D. A., Fischer, E. V., Baltensperger, U., Weingartner, E., Coen, M. C., Sharma, S., Macdonald, A. M., Leaitch, W. R., Lin, N.-H., Laj, P., Arsov, T., Kalapov, I., Jefferson, A., and Sheridan, P.: Climatology of aerosol radiative properties in the free troposphere, Atmos. Res., 102, 365–393, doi:10.1016/j.atmosres.2011.08.017, 2011.

Arnott, W. P., Hamasha, K., Moosmüller, H., Sheridan, P. J., and Ogren, J. A.: Towards aerosol light-absorption measurements with a 7-wavelength aethalometer: evaluation with a photoacoustic instrument and 3-wavelength nephelometer, Aerosol Sci. Tech., 39, 17–29, doi:10.1080/027868290901972, 2005.

Baars, H., Ansmann, A., Engelmann, R., and Althausen, D.: Continuous monitoring of the boundary-layer top with lidar, Atmos. Chem. Phys., 8, 7281–7296, doi:10.5194/acp-8-7281-2008, 2008.

Bond, T. C. and Bergstrom, R. W.: Light absorption by carbonaceous particles: an investigative review, Aerosol Sci. Tech., 40, 27–67, 2006.

Bond, T. C., Habib, G., and Bergstrom, R. W.: Limitations in the enhancement of visible light absorption due to mixing state, J. Geophys. Res.-Atmos., 111, 2156–2202, doi:10.1029/2006JD007315, 2006.

ACPD
14, 27731–27767, 2014

Boulon, J., Sellegri, K., Hervo, M., Picard, D., Pichon, J.-M., Fréville, P., and Laj, P.: Investigation of nucleation events vertical extent: a long term study at two different altitude sites, Atmos. Chem. Phys., 11, 5625–5639, doi:10.5194/acp-11-5625-2011, 2011.

Bourcier, L., Sellegri, K., Chausse, P., Pichon, J., and Laj, P.: Seasonal variation of water-soluble inorganic components in aerosol size-segregated at the puy de Dôme station (1465 m a.s.l.), France, J. Atmos. Chem., 69, 47–66, doi:10.1007/s10874-012-9229-2, 2012.

Brooks, I. M.: Finding boundary layer top: application of a wavelet covariance transform to lidar backscatter profiles, J. Atmos. Ocean. Tech., 20, 1092–1105, doi:10.1175/1520-0426(2003)020<1092:FBLTAO>2.0.CO;2, 2003.

Bukowiecki, N., Zieger, P., Weingartner, E., Jurányi, Z., Gysel, M., Neininger, B., Schneider, B., Hueglin, C., Ulrich, A., Wichser, A., Henne, S., Brunner, D., Kaegi, R., Schwikowski, M., Tobler, L., Wienhold, F. G., Engel, I., Buchmann, B., Peter, T., and Baltensperger, U.: Ground-based and airborne in-situ measurements of the Eyjafjallajökull volcanic aerosol plume in Switzerland in spring 2010, Atmos. Chem. Phys., 11, 10011–10030, doi:10.5194/acp-11-10011-2011, 2011.

Burkart, J., Steiner, G., Reischl, G., Moshammer, H., Neuberger, M., and Hitzenberger, R.: Characterizing the performance of two optical particle counters (Grimm OPC1.108 and OPC1.109) under urban aerosol conditions, J. Aerosol Sci., 41, 953–962, doi:10.1016/j.jaerosci.2010.07.007, 2010.

Carrico, C. M., Rood, M. J., Ogren, J. A., Neusüß, C., Wiedensohler, A., and Heintzenberg, J.: Aerosol Optical properties at Sagres, Portugal during ACE-2, Tellus B, 52, 694–715, doi:10.1034/j.1600-0889.2000.00049.x, 2000.

Cheng, Y. F., Wiedensohler, A., Eichler, H., Heintzenberg, J., Tesche, M., Ansmann, A., Wendisch, M., Su, H., Althausen, D., Herrmann, H., Gnauk, T., Brüggemann, E., Hu, M., and Zhang, Y. H.: Relative humidity dependence of aerosol optical properties and direct radiative forcing in the surface boundary layer at Xinken in Pearl River Delta of China: an observation based numerical study, Atmos. Environ., 42, 6373–6397, doi:10.1016/j.atmosenv.2008.04.009, 2008.

Chylek, P. and Wong, J.: Effect of absorbing aerosols on global radiation budget, Geophys. Res. Lett., 22, 929–931, doi:10.1029/95GL00800, 1995.

Collaud Coen, M., Weingartner, E., Nyeki, S., Cozic, J., Henning, S., Verheggen, B., Gehrig, R., and Baltensperger, U.: Long-term trend analysis of aerosol variables at the high-alpine site Jungfraujoch, J. Geophys. Res., 112, D13213, doi:10.1029/2006jd007995, 2007.

ACPD
14, 27731–27767, 2014

Collaud Coen, M., Weingartner, E., Apituley, A., Ceburnis, D., Fierz-Schmidhauser, R., Flentje, H., Henzing, J. S., Jennings, S. G., Moerman, M., Petzold, A., Schmid, O., and Baltensperger, U.: Minimizing light absorption measurement artifacts of the Aethalometer: evaluation of five correction algorithms, Atmos. Meas. Tech., 3, 457–474, doi:10.5194/amt-3-457-2010, 2010.

Collaud Coen, M., Andrews, E., Asmi, A., Baltensperger, U., Bukowiecki, N., Day, D., Fiebig, M., Fjaeraa, A. M., Flentje, H., Hyvärinen, A., Jefferson, A., Jennings, S. G., Kouvarakis, G., Lihavainen, H., Lund Myhre, C., Malm, W. C., Mihapopoulos, N., Molenar, J. V., O'Dowd, C., Ogren, J. A., Schichtel, B. A., Sheridan, P., Virkkula, A., Weingartner, E., Weller, R., and Laj, P.: Aerosol decadal trends – Part 1: In-situ optical measurements at GAW and IMPROVE stations, Atmos. Chem. Phys., 13, 869–894, doi:10.5194/acp-13-869-2013, 2013.

Covert, D. S., Charlson, R. J., and Ahlquist, N. C.: A study of the relationship of chemical composition and humidity to light scattering by aerosols, J. Appl. Meteorol., 11, 968–976, doi:10.1175/1520-0450(1972)011<0968:ASOTRO>2.0.CO;2, 1972.

Delene, D. J. and Ogren, J. A.: Variability of aerosol optical properties at four North American surface monitoring sites, J. Atmos. Sci., 59, 1135–1150, doi:10.1175/1520-0469(2002)059<1135:VOAOPA>2.0.CO;2, 2002.

Draxler, R. R. and Rolph, G. D.: HYSPLIT (HYbrid Single-Particle Lagrangian Integrated Trajectory) Model access via NOAA ARL READY Website, NOAA Air Resour. Lab., Silver Spring, MD, available at: http://ready.arl.noaa.gov/HYSPLIT.php, 2012.

Dubovik, O. and King, M. D.: A flexible inversion algorithm for retrieval of aerosol optical properties from Sun and sky radiance measurements, J. Geophys. Res.-Atmos., 105, 20673–20696, 2000.

Duplissy, J., Gysel, M., Sjogren, S., Meyer, N., Good, N., Kammermann, L., Michaud, V., Weigel, R., Martins dos Santos, S., Gruening, C., Villani, P., Laj, P., Sellegri, K., Metzger, A., McFiggans, G. B., Wehrle, G., Richter, R., Dommen, J., Ristovski, Z., Baltensperger, U., and Weingartner, E.: Intercomparison study of six HTDMAs: results and recommendations, Atmos. Meas. Tech., 2, 363–378, doi:10.5194/amt-2-363-2009, 2009.

Fierz-Schmidhauser, R., Zieger, P., Gysel, M., Kammermann, L., DeCarlo, P. F., Baltensperger, U., and Weingartner, E.: Measured and predicted aerosol light scattering enhancement factors at the high alpine site Jungfraujoch, Atmos. Chem. Phys., 10, 2319–2333, doi:10.5194/acp-10-2319-2010, 2010a.

ACPD
14, 27731–27767, 2014

Fierz-Schmidhauser, R., Zieger, P., Vaishya, A., Monahan, C., Bialek, J., O'Dowd, C. D., Jennings, S. G., Baltensperger, U., and Weingartner, E.: Light scattering enhancement factors in the marine boundary layer (Mace Head, Ireland), J. Geophys. Res., 115, D20204, doi:10.1029/2009jd013755, 2010b.

Freney, E. J., Sellegri, K., Canonaco, F., Boulon, J., Hervo, M., Weigel, R., Pichon, J. M., Colomb, A., Prévôt, A. S. H., and Laj, P.: Seasonal variations in aerosol particle composition at the puy-de-Dôme research station in France, Atmos. Chem. Phys., 11, 13047–13059, doi:10.5194/acp-11-13047-2011, 2011.

Gassó, S., Hegg, D. A., Covert, D. S., Collins, D., Noone, K. J., Öström, E., Schmid, B., Russell, P. B., Livingston, J. M., Durkee, P. A., and Jonsson, H.: Influence of humidity on the aerosol scattering coefficient and its effect on the upwelling radiance during ACE-2, Tellus B, 52, 546–567, 2000.

Gilbert, R. O.: Statistical Methods for Environmental Pollution Monitoring, John Wiley and Sons, 1987.

Hasan, H. and Dzubay, T. G.: Apportioning light extinction coefficients to chemical species in atmospheric aerosol, Atmos. Environ., 1967, 17, 1573–1581, doi:10.1016/0004-6981(83)90310-4, 1983.

Henne, S., Brunner, D., Folini, D., Solberg, S., Klausen, J., and Buchmann, B.: Assessment of parameters describing representativeness of air quality in-situ measurement sites, Atmos. Chem. Phys., 10, 3561–3581, doi:10.5194/acp-10-3561-2010, 2010.

Hervo, M., Quennehen, B., Kristiansen, N. I., Boulon, J., Stohl, A., Fréville, P., Pichon, J.-M., Picard, D., Labazuy, P., Gouhier, M., Roger, J.-C., Colomb, A., Schwarzenboeck, A., and Sellegri, K.: Physical and optical properties of 2010 Eyjafjallajökull volcanic eruption aerosol: ground-based, Lidar and airborne measurements in France, Atmos. Chem. Phys., 12, 1721–1736, doi:10.5194/acp-12-1721-2012, 2012.

Holmgren, H., Sellegri, K., Hervo, M., Rose, C., Freney, E., Villani, P., and Laj, P.: Hygroscopic properties and mixing state of aerosol measured at the high-altitude site Puy de Dôme (1465 m a.s.l.), France, Atmos. Chem. Phys., 14, 9537–9554, doi:10.5194/acp-14-9537-2014, 2014.

IPCC, Climate Change 2007: The Physical Science Basis, in: Contribution of Working Group I to the Fourth Assessment Report of the Intergovernmental Panel on Climate Change, edited by: Solomon, S., Qin, D., Manning, M., Chen, Z., Marquis, M., Averyt, K. B., Tignor, M., and Miller, H. L., Cambridge University Press, 996 pp, 2007.

ACPD
14, 27731–27767, 2014

IPCC, Climate Change 2013: The Physical Science Basis, in: Contribution of Working Group I to the Fifth Assessment Report of the Intergovern-mental Panel on Climate Change, edited by: Stocker, T. F., Qin, D., Plattner, G.-K., Tignor, M., Allen, S. K., Boschung, J., Nauels, A., Xia, Y., Bex, V., and Midgley, P. M., Cambridge University Press, 1535 pp, 2013.

Li-Jones, X., Maring, H. B., and Prospero, J. M.: Effect of relative humidity on light scattering by mineral dust aerosol as measured in the marine boundary layer over the tropical Atlantic Ocean, J. Geophys. Res., 103, 31113–31121, doi:10.1029/98JD01800, 1998.

Kalivitis, N., Bougiatioti, A., Kouvarakis, G., and Mihalopoulos, N.: Long term measurements of atmospheric aerosol optical properties in the Eastern Mediterranean, Atmos. Res., 102, 351–357, doi:10.1016/j.atmosres.2011.08.013, 2011.

Kotchenruther, R. A. and Hobbs, P. V.: Humidification factors of aerosols from biomass burning in Brazil, J. Geophys. Res., 103, 32081–32089, doi:10.1029/98JD00340, 1998.

Kotchenruther, R. A., Hobbs, P. V., and Hegg, D. A.: Humidification factors for atmospheric aerosols off the mid-Atlantic coast of the United States, J. Geophys. Res., 104, 2239–2251, doi:10.1029/98JD01751, 1999.

Laj, P., Klausen, J., Bilde, M., Plaß-Duelmer, C., Pappalardo, G., Clerbaux, C., Baltensperger, U., Hjorth, J., Simpson, D., Reimann, S., Coheur, P. F., Richter, A., De Mazière, M., Rudich, Y., McFiggans, G., Torseth, K., Wiedensohler, A., Morin, S., Schulz, M., Allan, J. D., Attié, J. L., Barnes, I., Birmili, W., Cammas, J. P., Dommen, J., Dorn, H. P., Fowler, D., Fuzzi, S., Glasius, M., Granier, C., Hermann, M., Isaksen, I. S. A., Kinne, S., Koren, I., Madonna, F., Maione, M., Massling, A., Moehler, O., Mona, L., Monks, P. S., Müller, D., Müller, T., Orphal, J., Peuch, V. H., Stratmann, F., Tanré, D., Tyndall, G., Abo Riziq, A., Van Roozendael, M., Villani, P., Wehner, B., Wex, H., and Zardini, A. A.: Measuring atmospheric composition change, Atmos. Environ., 43, 5351–5414, doi:10.1016/j.atmosenv.2009.08.020, 2009.

Lesins, G., Chylek, P., and Lohmann, U.: A study of internal and external mixing scenarios and its effect on aerosol optical properties and direct radiative forcing, J. Geophys. Res., 107, 4094, doi:10.1029/2001JD000973, 2002.

Lyamani, H., Olmo, F. J., and Alados-Arboledas, L.: Physical and optical properties of aerosols over an urban location in Spain: seasonal and diurnal variability, Atmos. Chem. Phys., 10, 239–254, doi:10.5194/acp-10-239-2010, 2010.

ACPD
14, 27731–27767, 2014

Mallet, M., Roger, J. C., Despiau, S., Dubovik, O., and Putaud, J. P.: Microphysical and optical properties of aerosol particles in urban zone during ESCOMPTE, Atmos. Res., 69, 73–97, doi:10.1016/j.atmosres.2003.07.001, 2003.

Marcq, S., Laj, P., Roger, J. C., Villani, P., Sellegri, K., Bonasoni, P., Marinoni, A., Cristofanelli, P., Verza, G. P., and Bergin, M.: Aerosol optical properties and radiative forcing in the high Himalaya based on measurements at the Nepal Climate Observatory-Pyramid site (5079 m a.s.l.), Atmos. Chem. Phys., 10, 5859–5872, doi:10.5194/acp-10-5859-2010, 2010.

Mattis, I., Müller, D., Ansmann, A., Wandinger, U., Preißler, J., Seifert, P., and Tesche, M.: Ten years of multiwavelength Raman lidar observations of free-tropospheric aerosol layers over central Europe: geometrical properties and annual cycle, J. Geophys. Res., 113, D20202, doi:10.1029/2007jd009636, 2008.

Mätzler, C.: MATLAB Functions for Mie Scattering and Absorption, Res. Rep. 2002–2008, Inst. Für Angew. Phys., Bern, 2002.

McKendry, I. G., Strawbridge, K. B., O'Neill, N. T., Macdonald, A. M., Liu, P. S. K., Leaitch, W. R., Anlauf, K. G., Jaegle, L., Fairlie, T. D., and Westphal, D. L.: Trans-Pacific transport of Saharan dust to western North America: a case study, J. Geophys. Res., 112, D01103, doi:10.1029/2006JD007129, 2007.

Michel Flores, J., Bar-Or, R. Z., Bluvshtein, N., Abo-Riziq, A., Kostinski, A., Borrmann, S., Koren, I., Koren, I., and Rudich, Y.: Absorbing aerosols at high relative humidity: linking hygroscopic growth to optical properties, Atmos. Chem. Phys., 12, 5511–5521, doi:10.5194/acp-12-5511-2012, 2012.

Nessler, R., Weingartner, E., and Baltensperger, U.: Effect of humidity on aerosol light absorption and its implications for extinction and the single scattering albedo illustrated for a site in the lower free troposphere, J. Aerosol Sci., 36, 958–972, doi:10.1016/j.jaerosci.2004.11.012, 2005.

Petters, M. D. and Kreidenweis, S. M.: A single parameter representation of hygroscopic growth and cloud condensation nucleus activity, Atmos. Chem. Phys., 7, 1961–1971, doi:10.5194/acp-7-1961-2007, 2007.

Petzold, A., Schloesser, H., Sheridan, P. J., Arnott, W. P., Ogren, J. A., and Virkkula, A.: Evaluation of Multiangle Absorption Photometry for Measuring Aerosol Light Absorption, Aerosol Sci. Tech., 39, 40–51, 2005.

ACPD
14, 27731–27767, 2014

Pilinis, C., Pandis, S. N., and Seinfeld, J. H.: Sensitivity of direct climate forcing by atmospheric aerosols to aerosol size and composition, J. Geophys. Res., 100, 18739–18754, doi:10.1029/95JD02119, 1995.

Raut, J.-C. and Chazette, P.: Retrieval of aerosol complex refractive index from a synergy between lidar, sunphotometer and in situ measurements during LISAIR experiment, Atmos. Chem. Phys., 7, 2797–2815, doi:10.5194/acp-7-2797-2007, 2007.

Schladitz, A., Müller, T., Nordmann, S., Tesche, M., Groß, S., Freudenthaler, V., Gasteiger, J., and Wiedensohler, A.: In situ aerosol characterization at Cape Verde, Tellus B, 63, 549–572, doi:10.1111/j.1600-0889.2011.00568.x, 2011.

Schmid, O., Artaxo, P., Arnott, W. P., Chand, D., Gatti, L. V., Frank, G. P., Hoffer, A., Schnaiter, M., and Andreae, M. O.: Spectral light absorption by ambient aerosols influenced by biomass burning in the Amazon Basin. I: Comparison and field calibration of absorption measurement techniques, Atmos. Chem. Phys., 6, 3443–3462, doi:10.5194/acp-6-3443-2006, 2006.

Stock, M., Cheng, Y. F., Birmili, W., Massling, A., Wehner, B., Müller, T., Leinert, S., Kalivitis, N., Mihalopoulos, N., and Wiedensohler, A.: Hygroscopic properties of atmospheric aerosol particles over the Eastern Mediterranean: implications for regional direct radiative forcing under clean and polluted conditions, Atmos. Chem. Phys., 11, 4251–4271, doi:10.5194/acp-11-4251-2011, 2011.

Tang, I. N.: Chemical and size effects of hygroscopic aerosols on light scattering coefficients, J. Geophys. Res., 101, 19245–19,250, doi:10.1029/96JD03003, 1996.

Venzac, H., Sellegri, K., Villani, P., Picard, D., and Laj, P.: Seasonal variation of aerosol size distributions in the free troposphere and residual layer at the puy de Dôme station, France, Atmos. Chem. Phys., 9, 1465–1478, doi:10.5194/acp-9-1465-2009, 2009.

Villani, P., Picard, D., Michaud, V., Laj, P., and Wiedensohler, A.: Design and validation of a volatility hygroscopic tandem differential mobility analyzer (VH-TDMA) to characterize the relationships between the thermal and hygroscopic properties of atmospheric aerosol particles, Aerosol Sci. Tech., 42, 729–741, doi:10.1080/02786820802255668, 2008.

Virkkula, A., Mäkelä, T., Hillamo, R., Yli-Tuomi, T., Hirsikko, A., Hämeri, K., and Koponen, I. K.: A simple procedure for correcting loading effects of aethalometer data, J. Air Waste Manage., 57, 1214–1222, doi:10.3155/1047-3289.57.10.1214, 2007.

ACPD
14, 27731–27767, 2014

Ward, D. and Cotton, W.: A method for forecasting cloud condensation nuclei using predictions of aerosol physical and chemical properties from WRF/Chem, J. Appl. Meteorol. Clim., 50, 1601–1615, doi:10.1175/2011JAMC2644.1, 2011.

Weingartner, E., Saathoff, H., Schnaiter, M., Streit, N., Bitnar, B., and Baltensperger, U.: Absorption of light by soot particles: determination of the absorption coefficient by means of aethalometers, J. Aerosol Sci., 34, 1445–1463, doi:10.1016/S0021-8502(03)00359-8, 2003.

Wiedensohler, A., Birmili, W., Nowak, A., Sonntag, A., Weinhold, K., Merkel, M., Wehner, B., Tuch, T., Pfeifer, S., Fiebig, M., Fjäraa, A. M., Asmi, E., Sellegri, K., Depuy, R., Venzac, H., Villani, P., Laj, P., Aalto, P., Ogren, J. A., Swietlicki, E., Williams, P., Roldin, P., Quincey, P., Hüglin, C., Fierz-Schmidhauser, R., Gysel, M., Weingartner, E., Riccobono, F., Santos, S., Grüning, C., Faloon, K., Beddows, D., Harrison, R., Monahan, C., Jennings, S. G., O'Dowd, C. D., Marinoni, A., Horn, H.-G., Keck, L., Jiang, J., Scheckman, J., McMurry, P. H., Deng, Z., Zhao, C. S., Moerman, M., Henzing, B., de Leeuw, G., Löschau, G., and Bastian, S.: Mobility particle size spectrometers: harmonization of technical standards and data structure to facilitate high quality long-term observations of atmospheric particle number size distributions, Atmos. Meas. Tech., 5, 657–685, doi:10.5194/amt-5-657-2012, 2012.

Yu, F., Luo, G., and Ma, X.: Regional and global modeling of aerosol optical properties with a size, composition, and mixing state resolved particle microphysics model, Atmos. Chem. Phys., 12, 5719–5736, doi:10.5194/acp-12-5719-2012, 2012.

Zhang, K., O'Donnell, D., Kazil, J., Stier, P., Kinne, S., Lohmann, U., Ferrachat, S., Croft, B., Quaas, J., Wan, H., Rast, S., and Feichter, J.: The global aerosol-climate model ECHAM-HAM, version 2: sensitivity to improvements in process representations, Atmos. Chem. Phys., 12, 8911–8949, doi:10.5194/acp-12-8911-2012, 2012.

Zhang, R., Khalizov, A. F., Pagels, J., Zhang, D., Xue, H., and McMurry, P. H.: Variability in morphology, hygroscopicity, and optical properties of soot aerosols during atmospheric processing, P. Natl. Acad. Sci. USA, 105, 10291–10296, doi:10.1073/pnas.0804860105, 2008.

Zieger, P., Fierz-Schmidhauser, R., Gysel, M., Ström, J., Henne, S., Yttri, K. E., Baltensperger, U., and Weingartner, E.: Effects of relative humidity on aerosol light scattering in the Arctic, Atmos. Chem. Phys., 10, 3875–3890, doi:10.5194/acp-10-3875-2010, 2010.

Zieger, P., Weingartner, E., Henzing, J., Moerman, M., de Leeuw, G., Mikkilä, J., Ehn, M., Petäjä, T., Clémer, K., van Roozendael, M., Yilmaz, S., Frieß, U., Irie, H., Wagner, T., Shaiganfar, R., Beirle, S., Apituley, A., Wilson, K., and Baltensperger, U.: Comparison of ambient aerosol extinction coefficients obtained from in-situ, MAX-DOAS and LIDAR measure-

ACPD
14, 27731–27767, 2014

ments at Cabauw, Atmos. Chem. Phys., 11, 2603–2624, doi:10.5194/acp-11-2603-2011, 2011.

Zieger, P., Kienast-Sjögren, E., Starace, M., von Bismarck, J., Bukowiecki, N., Baltensperger, U., Wienhold, F. G., Peter, T., Ruhtz, T., Collaud Coen, M., Vuilleumier, L., Maier, O., Emili, E., Popp, C., and Weingartner, E.: Spatial variation of aerosol optical properties around the high-alpine site Jungfraujoch (3580 m a.s.l.), Atmos. Chem. Phys., 12, 7231–7249, doi:10.5194/acp-12-7231-2012, 2012.

Zieger, P., Fierz-Schmidhauser, R., Weingartner, E., and Baltensperger, U.: Effects of relative humidity on aerosol light scattering: results from different European sites, Atmos. Chem. Phys., 13, 10609–10631, doi:10.5194/acp-13-10609-2013, 2013.

ACPD
14, 27731–27767, 2014

Table 1. Dry optical properties measured at 550 nm at PdD (2010–2011) (median (25th percentile–75th percentile)).

Night (0–6 h)								
Origin	σ_{sca} (M m^{-1})		σ_{abs}(M m^{-1})		ω0		g	
African	12.04	[0.67–42.18]	0.76	[0.10–3.67]	0.91	[0.82–0.94]	0.57	[0.31–0.62]
Oceanic	5.32	[0.36–25.20]	0.39	[0.07–2.03]	0.92	[0.80–0.95]	0.55	[0.28–0.63]
Oceanic Mod	12.93	[0.63–59.5]	0.84	[0.10–3.28]	0.93	[0.86–0.96]	0.57	[0.17–0.64]
Continental	21.92	[1.40–126.23]	1.60	[0.22–5.49]	0.92	[0.84–0.96]	0.60	[0.37–0.68]
Local	20.25	[2.61–50.88]	1.72	[0.22–3.68]	0.90	[0.85–0.94]	0.58	[0.46–0.63]
All	11.59	[0.49–53.26]	0.80	[0.09–3.42]	0.92	[0.84–0.95]	0.57	[0.30–0.65]
Day (12–18 h)								
Origin	σ_{sca} (M m^{-1})		σ_{abs}(M m^{-1})		ω0		g	
African	15.83	[1.89–44.60]	1.43	[0.23–4.70]	0.89	[0.78–0.94]	0.56	[0.40–0.62]
Oceanic	8.14	[0.48–32.91]	0.72	[0.11–3.16]	0.90	[0.79–0.96]	0.55	[0.29–0.62]
Oceanic Mod	16.86	[2.10–45.39]	1.12	[0.18–3.69]	0.91	[0.79–0.96]	0.56	[0.43–0.63]
Continental	26.47	[2.08–147.94]	2.11	[0.37–8.68]	0.92	[0.78–0.96]	0.60	[0.42–0.69]
Local	20.56	[3.32–53.53]	2.75	[0.44–5.98]	0.87	[0.72–0.93]	0.55	[0.43–0.63]
All	14.94	[0.92–60.58]	1.28	[0.17–4.72]	0.90	[0.78–0.95]	0.56	[0.39–0.65]

ACPD
14, 27731–27767, 2014

Table 1. Continued.

Night (0–6 h)				
Origin		mr		mi
African	1.425	[1.360–1.590]	0.011	[0.005–0.029]
Oceanic	1.45	[1.350–1.550]	0.011	[0.001–0.041]
Oceanic Mod	1.405	[1.369–1.533]	0.008	[0.003–0.024]
Continental	1.43	[1.352–1.556]	0.01	[0.004–0.022]
Local	1.405	[1.361–1.547]	0.01	[0.006–0.016]
All	1.43	[1.360–1.550]	0.01	[0.001–0.032]
Day (12–18 h)				
Origin		mr		mi
African	1.43	[1.360–1.590]	0.012	[0.006–0.030]
Oceanic	1.43	[1.350–1.550]	0.011	[0.001–0.041]
Oceanic Mod	1.42	[1.369–1.533]	0.01	[0.001–0.032]
Continental	1.43	[1.352–1.556]	0.01	[0.005–0.039]
Local	1.415	[1.361–1.547]	0.014	[0.007–0.029]
All	1.43	[1.360–1.550]	0.011	[0.004–0.039]

ACPD
14, 27731–27767, 2014

Table 2. Fitting coefficients of the calculated hygroscopic scattering enhancement factor parameterization as a function of RH for different air masses.

	a_1	a_2	a_3	a_4
African	9.36E-01	5.23E-03	1.55E-06	1.49E-01
Oceanic	9.18E-01	6.08E-03	3.10E-07	1.68E-01
Oceanic Mod	9.88E-01	5.14E-03	8.66E-04	8.82E-02
Continental	9.69E-01	3.50E-03	6.02E-05	1.07E-01
Local	9.18E-01	6.05E-03	6.17E-07	1.60E-01

ACPD
14, 27731–27767, 2014

Table 3. Hygroscopic optical enhancement at 550 nm and 90 % RH calculated from PdD data for different air masses (2010–2011) (median (25th percentile–75th percentile)).

	$f\sigma$abs		$f\omega$0		$f g$	
African	1.10	[0.97–1.30]	1.06	[1.015–1.131]	1.10	[1.025–1.194]
Oceanic	1.12	[0.97–1.56]	1.07	[1.008–1.156]	1.11	[1.013–1.237]
Oceanic Mod	1.14	[0.89–1.66]	1.05	[1.018–1.131]	1.15	[1.051–1.251]
Continental	1.08	[0.89–1.35]	1.04	[1.014–1.142]	1.10	[1.033–1.193]
Local	1.10	[0.93–1.65]	1.06	[1.021–1.107]	1.10	[1.031–1.198]
All	1.11	[0.930–1.42]	1.05	[1.014–1.134]	1.11	[1.027–1.212]

ACPD
14, 27731–27767, 2014

Table 4. Climatology of the direct radiative forcing enhancement at 90 % humidity (Median (25th percentile–75th percentile)). These values are calculated from measurements at 550 nm at PdD for different air masses.

	$f\Delta F$	
African	2.9	[1.3–6.5]
Oceanic	3.1	[1.1–7.0]
Oceanic Mod	4.2	[1.5–8.2]
Continental	2.4	[1.3–6.3]
Local	2.8	[1.3–4.5]
All	2.8	[1.2–6.7]

ACPD
14, 27731–27767, 2014

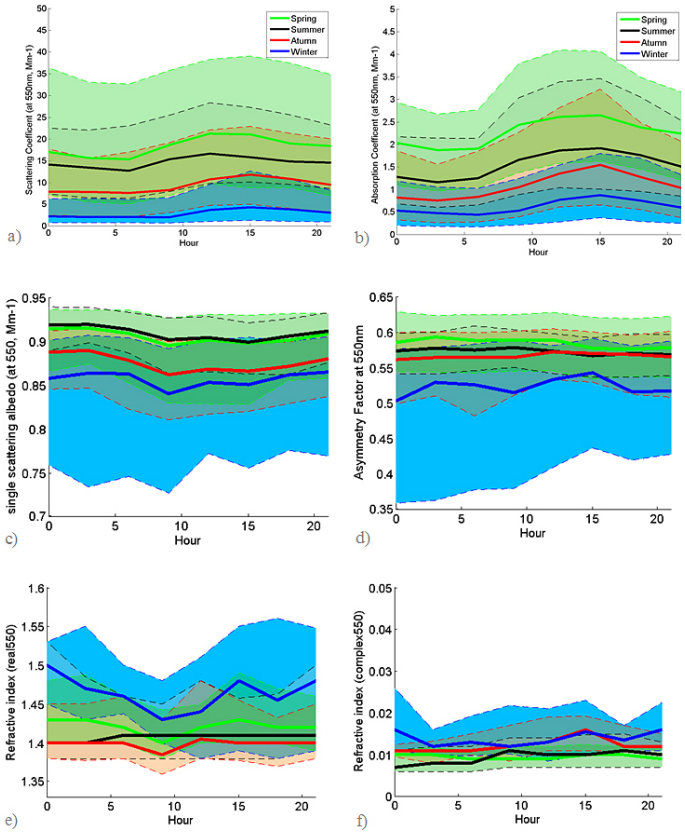

Figure 1. Diurnal variations of the optical properties at 550 nm for different seasons at the PdD: **(a)** scattering coefficient, **(b)** absorption coefficient, **(c)** single scattering albedo, **(d)** asymmetry factor, **(e)** real refractive index, **(f)** imaginary refractive index. The green curve corresponds to spring, the black to summer, the red to autumn and the blue to winter. The shaded areas are the regions between the 25th and the 75th percentile associated with the 4 curves. (**a–d**: 2008–2012, **e**, **f**: 2010–2012)

ACPD
14, 27731–27767, 2014

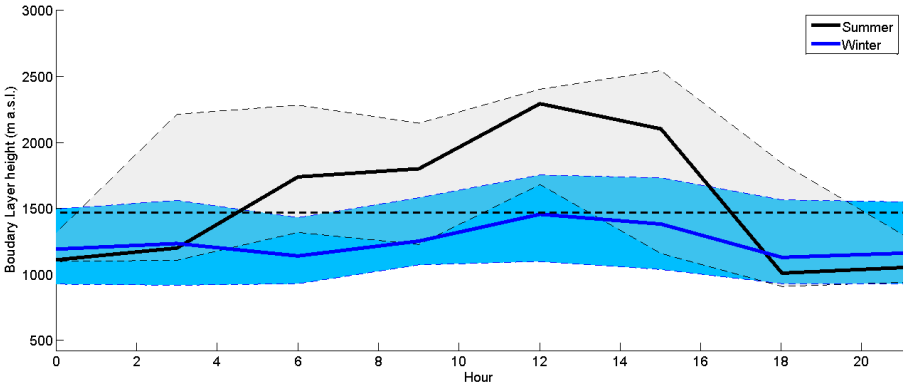

Figure 2. Mean planetary boundary layer height calculated from Lidar data of 2011. The black boundary layer line is the hourly median in summer and the blue the median in winter. The shaded area is the region between the 25th and the 75th percentile associated with the 2 curves. The black dashed line represent the height of the PdD (1465 m).

ACPD
14, 27731–27767, 2014

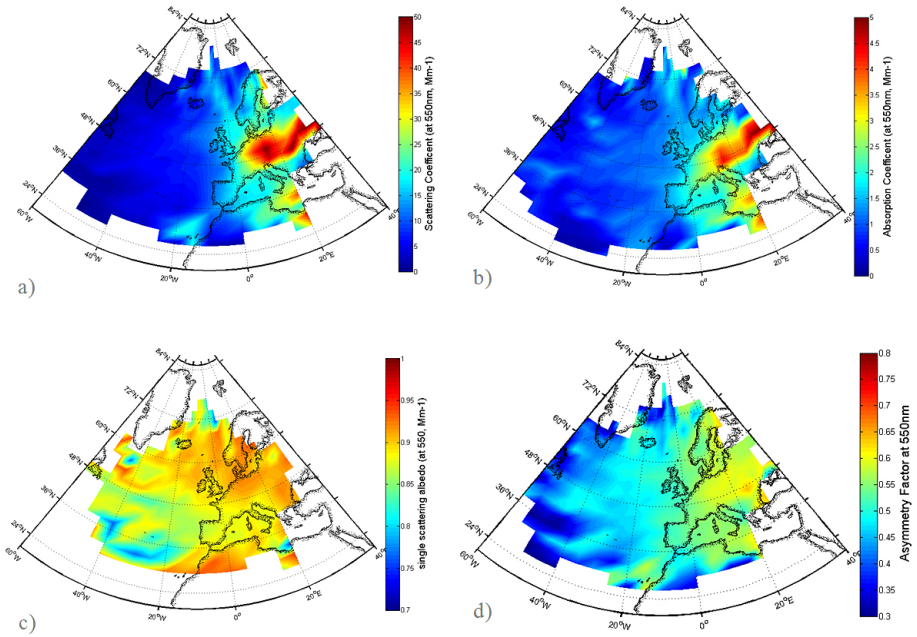

Figure 3. Map of the influence of the air mass origin on the optical properties at the PdD. **(a)** Scattering coefficient at 550 nm, **(b)** absorption coefficient, **(c)** single scattering albedo, **(d)** asymmetry factor. The maps are realized by combining measurements at 550 nm at the PdD and Hysplit back trajectories over the period 2008–2012.

ACPD
14, 27731–27767, 2014

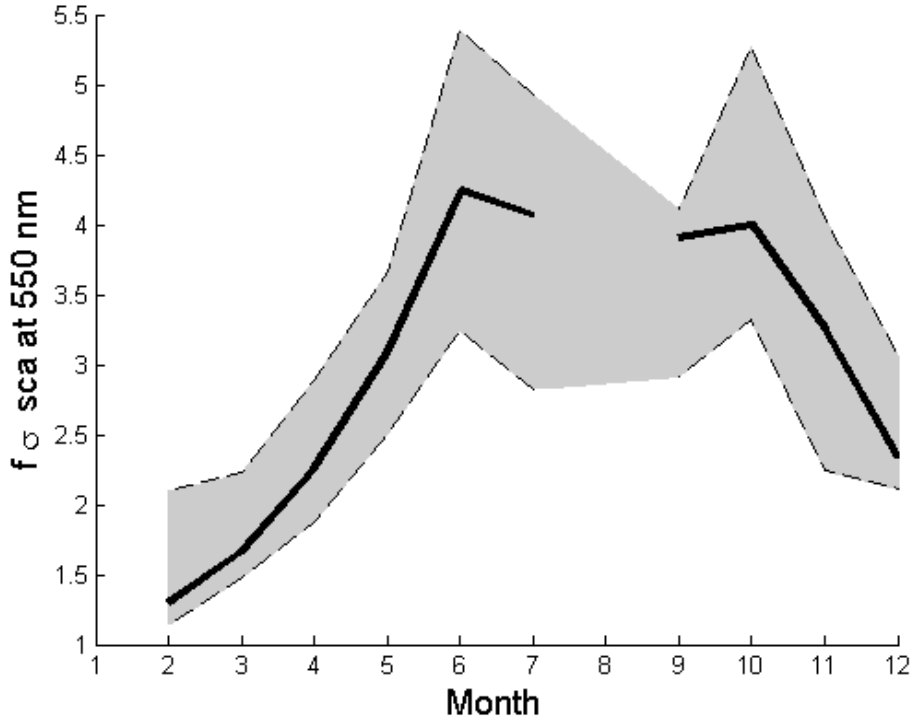

Figure 4. Seasonal evolution of the scattering enhancement factor calculated at 90 % RH. The shade area is the region between the 25th and the 75th percentile associated with the black curves.

ACPD
14, 27731–27767, 2014

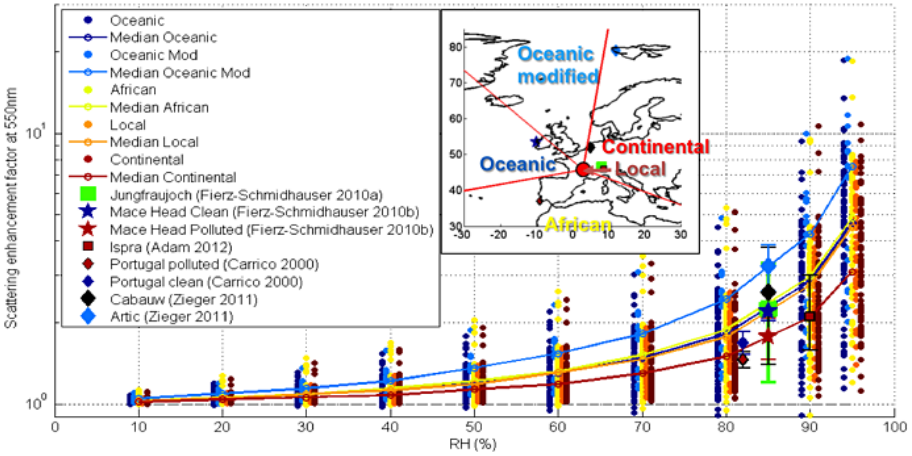

Figure 5. Humidogram of the calculated scattering enhancement factor at the PdD for different origins of air masses. The measurements available in the literature and their uncertainties are also shown. The colours represent the origin of the air mass. The median values for each air mass at different humidity are represented as lines.

ACPD
14, 27731–27767, 2014